

Article

Energy Efficiency and Throughput Maximization Using Millimeter Waves–Microwaves HetNets

Sonain Jamil ¹, MuhibUr Rahman ^{2,*}, Jawad Tanveer ³ and Amir Haider ^{4,*}¹ Department of Electronics Engineering, Sejong University, Seoul 05600, Korea; sonainjamil@sju.ac.kr² Department of Electrical Engineering, Polytechnique Montreal, Montreal, QC H3T 1J4, Canada³ School of Optical Engineering, Sejong University, Seoul 05600, Korea; jawadtanveer@sju.ac.kr⁴ Department of Intelligent Mechatronics Engineering, Sejong University, Seoul 05600, Korea

* Correspondence: muhibur.rahman@polymtl.ca (M.R.); amirhaider@sejong.ac.kr (A.H.)

Abstract: The deployment of millimeter waves can fulfil the stringent requirements of high bandwidth and high energy efficiency in fifth generation (5G) networks. Still, millimeter waves communication is challenging because it requires line of sight (LOS). The heterogeneous network (HetNet) of millimeter waves and microwaves solves this problem. This paper proposes a millimeter -microwaves heterogeneous HetNet deployed in an indoor factory (InF). In InF, the manufacturing and production are performed inside big and small halls. We consider non standalone dual-mode base stations (DMBS) working on millimeter waves and microwaves. We analyze the network in terms of throughput and energy efficiency (EE). We formulate mixed-integer-non-linear-programming (MINLP) to maximize the throughput and EE of the network. The formulated problem is a complex optimization problem and hard to solve with exhaustive search. We propose a novel outer approximation algorithm (OAA) to solve this problem, and the proposed algorithm OAA achieves optimal solution at $\beta = 10^{-3}$. At this β , the average throughput value obtained is approximately 50 Mbps, whereas the value of EE is 4.4 Mbits/J. We also compare the performance of OAA with the mesh-adaptive-direct-search-algorithm (NOMAD), and the experimental results verify that OAA outperforms NOMAD in terms of throughput and EE maximization. We also compare the performance of OAA with particle swarm optimization (PSO), genetic algorithm (GA), and many others optimization algorithms. Experimental results verify that OAA outperforms all other algorithms.

Keywords: optimization; resource allocation; millimeter waves; throughput; energy efficiency; HetNet



check for updates

Citation: Jamil, S.; Rahman, M.; Tanveer, J.; Haider, A. Energy Efficiency and Throughput Maximization Using Millimeter Waves–Microwaves HetNets. *Electronics* **2022**, *11*, 474. <https://doi.org/10.3390/electronics11030474>

Academic Editor: Enrique Rosales-Asensio

Received: 21 December 2021

Accepted: 3 February 2022

Published: 6 February 2022

Publisher's Note: MDPI stays neutral with regard to jurisdictional claims in published maps and institutional affiliations.



Copyright: © 2022 by the authors. Licensee MDPI, Basel, Switzerland. This article is an open access article distributed under the terms and conditions of the Creative Commons Attribution (CC BY) license (<https://creativecommons.org/licenses/by/4.0/>).

1. Introduction

The past few years have shown that millimeter-wave deployment can fulfil the spectrum shortage requirement for 5G [1]. The mm-wave has an unlicensed band of 60 GHz [2]. It opens the door for future correspondence utilizing channel transfer speed past 1 GHz [3], and this is the motivation behind 5G research committees and working groups effectively contributing huge research endeavors towards utilizing the mm-waves in cellular networks [4].

The mm-waves communication requires LOS, and the availability of LOS is one of the biggest challenges for mm-wave communication. These waves face the challenge of interference due to attenuation at shorter distances due to shorter ranges. However, reducing the interference effect due to attenuation at shorter distances improves transmission quality. An outdoor propagation environment produces rich multi-paths at 28 GHz. These multi-paths can be utilized to receive signal power, particularly in the case of non-line of sight (NLOS) [5]. Intelligent antennas with directional beamforming improve the propagation [6].

The mm-waves have so many advantages such as broad bandwidth, high data rate, and low latency to fulfil the requirements of future 5G networks, but mm-wave communi-

cation is highly challenging. The reason behind this is the requirement of the LOS, and to overcome this challenge in an indoor factory (InF), the mm-wave- μ wave HetNet is used. To deploy these HetNets, parameters such as throughput, EE, latency, and reliability must be considered. The greenhouse effect is caused by the emission of carbon dioxides (CO₂) from factories due to energy consumption. An increase in energy consumption increases the operational expenditure (OPEX) of the network. The other reasons for the rise in energy consumption are high data rates and dense deployment of base stations. These concerns have highlighted the need for energy-efficient resource allocation strategies for HetNets, reducing energy consumption while high-quality service standards are met.

This paper considers the InF scenario with mm-wave- μ wave HetNet. The primary objective is to increase the throughput and EE of this mm-wave- μ wave HetNet. The use of μ wave will improve EE and network throughput and be an appropriate solution to problems such as line of sight in mm-wave communication.

The following is the paper organization: Section 1 describes the introduction. Section 2 explains the work associated with the paper and its contributions. In Section 3, a system model is defined with problem solving and algorithm description. Section 4 illustrates the experimental results. Finally, Section 5 summarizes the entire work in the conclusion.

2. Related Work

Ansari et al. illustrated a scheme based on control database separation architecture (CDSA) which comprised a control base station (CBS) overlaying on database base station (DBS) [7]. They formulated an optimization problem having multiple objectives to improve energy and spectral efficiency. In Reference [8], the writers demonstrated the use of a recurrent neural network (RNN) and support vector machine (SVM) for resource allocation. In Reference [9], the authors assigned power in HetNets by using a convolutional neural network (CNN) which demands 6.76% of central processing unit (CPU) runtime. Similarly, the authors in [10], used CNN for the security analysis of the Internet-of-Things (IoT) enabled network and achieved 20% gain in precision. Chergui et al. proposed SVM based framework for semi-blind decoupling of uplink and downlink in sub-6 GHz band [11]. This method achieved an accuracy of 95%.

In Reference [12], the authors used Q-learning to minimize latency in mm-wave- μ waves HetNets. However, their model is limited to overhead beam preparation, which enhances the risk of failure. The writers of [13] suggested traditional infrastructure and medium access control (MAC) layer convergence for ultra-reliability and low latency of HetNet. However, this system fails to perform well in MIMO situations. In Reference [14], the authors propose a framework to enhance the throughput in the mm-wave communication network. This framework is based on game theory and is valid for short-range communication only. In Reference [15], the authors used extreme gradient boosting (XG-Boost) to improve the handovers success rate in HetNets. This technique had the drawback of service degradation during handovers. In Reference [16], Okamoto et al. proposed an online learning-based adaptive regularization of weight vectors (AROW) algorithm to find the throughput of HetNets. This scheme was only applicable to networks with throughput limited to 1 Gbit/s.

In Reference [17], game theory maximized data rate and energy utilization in HetNets. The network did not work well beyond a certain specified distance outside the same radius; the interference signal plus the noise ratio (SINR) decreased, which reduced efficiency. In Reference [18], a joint resource allocation algorithm (JRAA) and a greedy algorithm were put forward to maximize data rate in HetNets. The suggested framework utilized E-band and V-band, and the LTE band for resource allocation. In Reference [19], SVM based user allocation algorithm and alternating direction method of multipliers (ADMM) were recommended to make HetNets ultra-reliable with low latency. Both these algorithms were low complexity phase heuristic solutions. The network efficiency decayed with a sudden increase in the number of users. In Reference [20], exhaustive search and greedy zero-forcing dirty paper algorithms were utilized to maximize throughput in HetNets.

However, this technique was only applicable to the selection of multi-users in MMIMO orthogonal frequency division multiple access (OFDMA) networks. An efficient method to improve the EE of mm-wave- μ wave HetNet is proposed [21]. In this method, constraints such as interruption, power, and network rate are considered. The problem was solved by using the matching game approach.

Likewise, an algorithm was demonstrated in [22] to create mm-wave- μ wave HetNet more effectively when considering power limitations, interruption, and LOS. However, this method was better suited to massive MIMO. Similarly, in Reference [23], the DBMBOLA algorithm was proposed to maximize the EE in mm-wave- μ wave HetNet. The shortcomings of QoS were considered in this strategy. In Reference [24], the energy-efficient power allocation (EEPA) algorithm was proposed for EE in an mm-wave network. This algorithm was based on enhanced non-orthogonal multiple access (E-NOMA). The major drawback of this algorithm was that it did not apply to HetNets. In Reference [25], the authors enhanced the performance of HetNets considering the restrictions of path loss, power use, and LOS. The suggested algorithm is applied to the dense implementation of the mm-wave self-backhauled network. The authors in [26] demonstrated a signal-to-interference ratio-based algorithm to optimize throughput in an mm-wave network termed heuristic interference mitigation (HIM) algorithm. Similarly, in Reference [27], a heuristic algorithm (HUA) was proposed to increase the coverage and capacity of mm-wave- μ wave HetNet. QoS constraints were considered in this scheme, but mm-wave propagation problems such as path loss, rain fading, and LOS were ignored. Furthermore, the advantage of using a bag of features (BoF) to train classifiers such as SVM is illustrated in [28].

Mesodiakaki et al. in Reference [29] proposed the heuristic algorithm to maximize the EE and spectral efficiency of the mm-wave small cell network. However, the authors only focused on the small cell. Similarly, in Reference [30], the authors proposed a low complexity algorithm for the resource allocation in 5G HetNets. The proposed algorithm achieved optimal performance for the 3GPP scenarios. However, no existing studies have considered an InF scenario in which several robots, machines, and humans communicate with each other inside a small or big hall. Table 1 shows the existing mm-wave resource allocation techniques.

After analyzing Table 1, we conclude that there is little work on millimeter-wave- μ wave HetNets in the literature. Still, the authors have not proposed an optimal solution that jointly maximizes EE and network throughput in the InF scenario. In InF, the deployment of HetNets is quite challenging, as several robots and machines are communicating with each other simultaneously. We formulate a MINLP problem and propose a novel algorithm to optimize throughput and EE. We have used a plethora of algorithms such as firefly algorithm (FA) [31], cuckoo search (CS) [32], PSO [33], artificial bee colony (ABC) [34], teaching learning-based optimization (TLBO) [35], social group optimization (SGO) [36], basic open-source non-linear mixed integer programming (BOMIN) [37], genetic algorithm (GA) [38], and exhaustive search (ES) to compare and validate the results of the proposed algorithm.

Contribution

Analyzing the literature, we conclude that no maximization method considers the joint optimization of EE and throughput using mm-wave- μ wave HetNets in InF scenario. Our main contributions are summarized below:

1. A mathematical formulation of a model for throughput and EE maximization.
2. A solution to the formulated problem using OAA.
3. Extensive evaluation of results for validation of our method.
4. Comparison of the proposed algorithm with existing state-of-the-art algorithms.

Table 1. Summary of the existing mm-wave resource allocation techniques.

| Ref. No. | Het Nets | mm-Waves | InF | Objective | Constraints | Sample Approach | Limitations |
|------------|----------|----------|-----|-------------------------------------|--|--|--|
| [11] | ☒ | ☒ | ☒ | Maximum reliability and low latency | LOS, path loss | Semi blind decoupling approach | Low accuracy with NLOS |
| [12] | ☒ | ☒ | ☒ | Resource allocation | QoS, CSI, QoE, LOS | Q-learning | Increased probability of outage due to beam overhead training |
| [13] | ☒ | ☒ | ☒ | Ultra-Reliable Low latency | Radio interference | Reinforcement learning- Q-learning | Applicable in C-plane and U-plane |
| [14] | ☒ | ☒ | ☒ | Throughput maximization | Beamwidth of transmitter and receiver, power | Scheduling algorithm | Network throughput decreased with increase in transmission beamwidth |
| [15] | ☒ | ☒ | ☒ | Throughput maximization | Beamwidth, power | Matching theory | Short range mm-wave scenarios |
| [16] | ☒ | ☒ | ☒ | Throughput estimation | Online learning | AROW algorithm | Applicable for throughput less than 1Gbps |
| [17] | ☒ | ☒ | ☒ | Data rate and energy utilization | Power, interference | Game theory | Worked within specified radius |
| [18] | ☒ | ☒ | ☒ | Data-rate maximization | Power exclusive pairing, minimum rate | Joint resource allocation algorithm and greedy algorithm | Used E-band, V-band, and LTE band for resource allocation |
| [20] | ☒ | ☒ | ☒ | Throughput maximization | Power, resource selection | Exhaustive search and greedy zero forcing dirty paper | Multiuser selection in MIMO-OFDMA |
| [21] | ☒ | ☒ | ☒ | EE maximization | Power, interference, network rate | Matching theory and matching game theory | Applicable to small cells only |
| [22] | ☒ | ☒ | ☒ | EE maximization | Power, interference, QoS | ARA algorithm | Based on massive MIMO |
| [23] | ☒ | ☒ | ☒ | EE maximization | Interference, power, LOS | DBMBOLA algorithm | Two tier massive MIMO HetNet with wireless backhaul |
| [24] | ☒ | ☒ | ☒ | EE maximization | Power, interference, QoS | EEPA algorithm | Based on E-NOMA |
| [25] | ☒ | ☒ | ☒ | Throughput maximization | LOS, interference, path loss | RAMA algorithm | Based on dense deployment of mm-wave-SBH |
| [26] | ☒ | ☒ | ☒ | Throughput maximization | LOS, interference, path loss, power | HIM algorithm | Based on SIR |
| [27] | ☒ | ☒ | ☒ | Coverage and capacity maximization | Interference, QoS | HUA algorithm | Lack of mm-wave propagation probabilities |
| [29] | ☒ | ☒ | ☒ | EE and SE maximization | Power, SINR, traffic | Heuristic algorithm | Only focused on small cell network |
| [30] | ☒ | ☒ | ☒ | User association | Power, LOS | Backhaul routing algorithm | Computationally complex approach |
| This paper | ☒ | ☒ | ☒ | EE and throughput maximization | Power, rate, LOS | OAA | Applicable to InF having dual mode base stations |

3. System Model and Problem Formulation

3.1. Scenario of Indoor Factory

This article considers an InF scenario, as illustrated in Figure 1. All the base stations deployed in the design are dual mode. When there is LOS, these base stations work on millimeter waves. However, when there is NLOS, these base stations shift to μ waves.

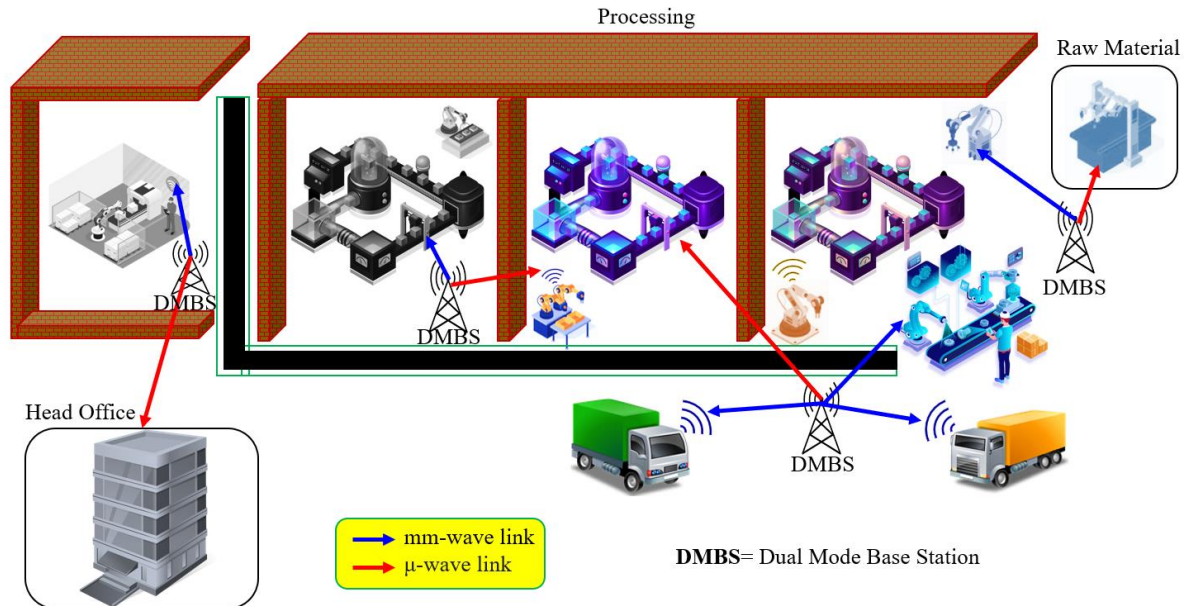


Figure 1. Smart factory scenario.

3.2. Indoor Factory (InF)

An InF is a smart factory based on the industrial internet of things (IIoT 4.0). The factory considered in this article has two types of halls in it. One type is a big hall, while the other is a small hall. The details about area and base station deployment in both arenas are described in Table 2:

Table 2. Abbreviations used for indoor factory scenario.

| Abbreviation | Description |
|--------------|---|
| InF | Indoor factory |
| InF-SL | Indoor factory with sparse clutter and low base station height |
| InF-SH | Indoor factory with sparse clutter and high base station height |
| InF-DL | Indoor factory with dense clutter and low base station height |
| InF-DH | Indoor factory with dense clutter and high base station height |
| DMBS | Dual mode base station |
| UE | User |

3.2.1. Big Hall of Indoor Factory

According to 3GPP Release 16 [39], the total area inhabited by one big hall of InF is 300 by 150 m². Each big gallery contains eighteen base stations. All the base stations are 50 m apart, and their height is 1.5 m and 8 m for InF-DL and InF-SH, respectively. The distribution of DMBS in the hall is illustrated in Figure 2.

3.2.2. Small Hall of Indoor Factory

According to 3GPP Release 16 [39], the total area inhabited by one small hall of InF is 120 by 60 m². Each big gallery contains eighteen base stations. All the base stations are 50 m

apart, and their height is 1.5 m and 8 m for InF-DL and InF-SH. The deployment of DMBS within the hall is illustrated in Figure 2. The height of the rooms having DMBS varies from five meters to ten meters. 3GPP Release 16 provides assessment factors for the InF.

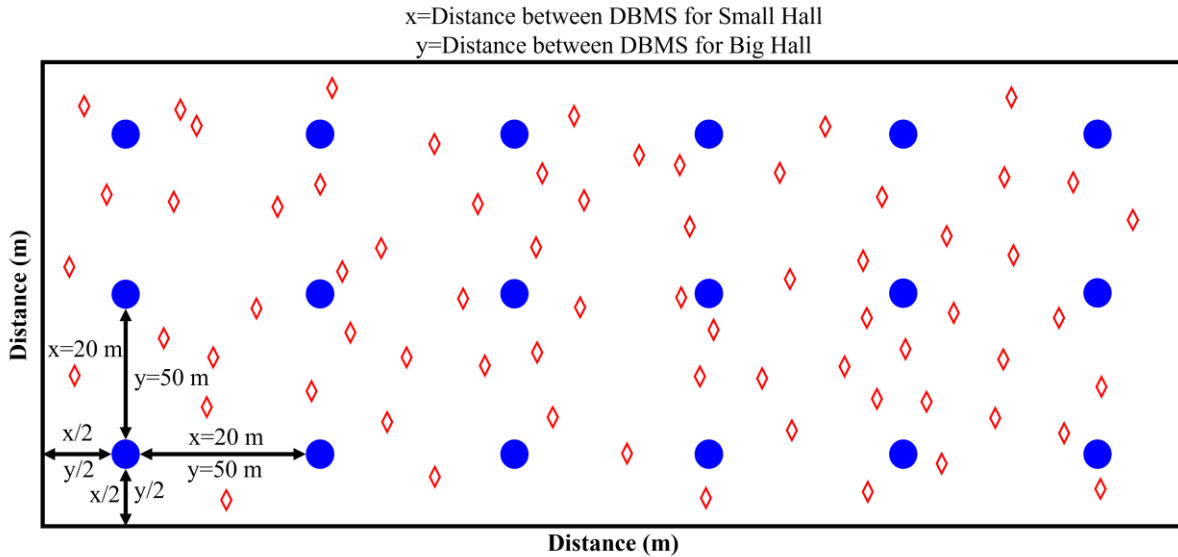


Figure 2. Simulation scenario in MATLAB; InF: Red diamond = UE, Blue circle = Dual-Mode Base Stations.

3.2.3. LOS and NLOS Path Loss

Equation (2) calculates the path loss of LOS, while path loss of NLOS in InF-SL, InF-DL, InF-SH, and InF-DH can be calculated by using Equations (4), (6), (8), and (10), respectively [39]. In these equations, d_{3D} is the distance between user (UE) and DMBS, and Equation (1) calculates d_{3D} , f_c is the central frequency normalized by 1 GHz [40].

$$d_{3D} = \sqrt{(d_{2D})^2 + (h_{BS} - h_{UT})^2}, \tag{1}$$

$$PL_{LOS} = 31.84 + 21.50 \log_{10}(d_{3D}) + 19.00 \log_{10}(f_c) \tag{2}$$

$$\text{InF-SL : PL} = 33.00 + 25.50 \log_{10}(d_{3D}) + 20.00 \log_{10}(f_c) \tag{3}$$

$$PL_{NLOS} = \max(PL, PL_{LOS}) \tag{4}$$

$$\text{InF-DL : PL} = 18.60 + 35.70 \log_{10}(d_{3D}) + 20.00 \log_{10}(f_c) \tag{5}$$

$$PL_{NLOS} = \max(PL, PL_{LOS}, PL_{\text{InF-SL}}) \tag{6}$$

$$\text{InF-SH : PL} = 32.40 + 23.00 \log_{10}(d_{3D}) + 20.00 \log_{10}(f_c) \tag{7}$$

$$PL_{NLOS} = \max(PL, PL_{LOS}) \tag{8}$$

$$\text{InF-DH : PL} = 33.63 + 21.90 \log_{10}(d_{3D}) + 20.00 \log_{10}(f_c) \tag{9}$$

$$PL_{NLOS} = \max(PL, PL_{LOS}) \tag{10}$$

3.2.4. Mathematical Model

In this article, an mm-waves- μ waves HetNet is considered. This network has \mathbf{M} links between UEs and DMBS. The time slot is shown in Figure 3. This time has two portions, including one for the alignment and the second for the data transmission.

3.2.5. Overhead of Alignment

Let T_p represents the pilot transmission time. The sector-level beamwidth for transmitter and receiver is represented by ψ_i^t and ψ_i^r , respectively, whereas beam-level beamwidth

for transmission and reception is denoted by φ_i^t and φ_i^r , respectively. Consequently, the overall duration for the alignment in a sector is given by Equation (11).

$$\tau_i(\varphi_i^t, \varphi_i^r) = \left\lceil \frac{\psi_i^t}{\varphi_i^t} \right\rceil \left\lceil \frac{\psi_i^r}{\varphi_i^r} \right\rceil T_P \tag{11}$$

where $\lceil \cdot \rceil$ denotes ceiling function. This function returns the smallest integer. The connection between transmitter and receiver is formed when the optimal directions are calculated after this data transmission begins. After the alignment process, any pair of DMBS and UE starts data communication. We derive continuous approximation τ_i by dumping the noncontinuous ceiling function. The latter cannot exceed the overall time T and can be excluded from the lower limit on possible bandwidth (12).

$$\varphi_i^t \varphi_i^r \geq \frac{T_P}{T} \psi_i^t \psi_i^r \tag{12}$$

Even though alignment happens within beamwidths at the sector level, we have $\varphi_i^t \leq \psi_i^t$ and $\varphi_i^r \leq \psi_i^r$. The transmission between DMBS and UEs is shown in Figure 4.

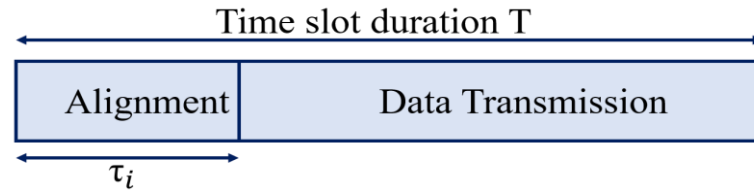


Figure 3. The segmentation of time slot for the i th link.

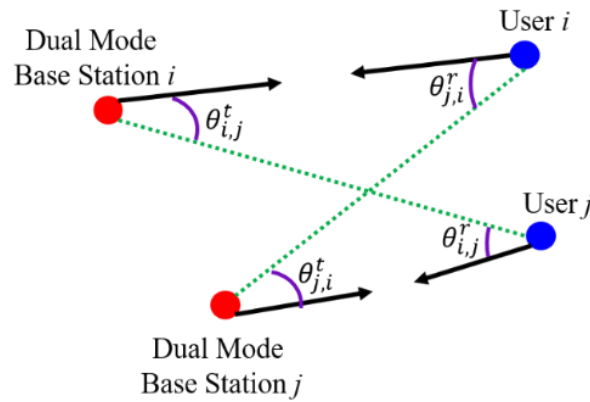


Figure 4. Transmission between DMBS and UEs.

3.2.6. The Effective Rate of Transmission

Let the channel gain be denoted by $g_c(i,j)$ for $DBMS_i$ and UE_j . Table 3 gives the summary of symbols used in a mathematical model. The transmitter and corresponding receiver gain can be determined by Equations (13) and (14) respectively.

$$g_{i,j}^t(\theta_{i,j}^t, \varphi_i^t) = \begin{cases} \frac{2\pi - (2\pi - \varphi_i^t)z}{\varphi_i^t}, & \text{if } |\theta_{i,j}^t| \leq \frac{\varphi_i^t}{2} \\ z, & \text{otherwise} \end{cases} \tag{13}$$

$$g_{i,j}^r(\theta_{i,j}^r, \varphi_i^r) = \begin{cases} \frac{2\pi - (2\pi - \varphi_i^r)z}{\varphi_i^r}, & \text{if } |\theta_{i,j}^r| \leq \frac{\varphi_i^r}{2} \\ z, & \text{otherwise} \end{cases} \tag{14}$$

Table 3. Description of symbols.

| Symbol | Description | Symbol | Description |
|-------------|---------------------------------------|-------------|--|
| φ^t | Beam level beamwidth of a transmitter | φ^r | Beam level beamwidth of the receiver |
| ψ^t | Sector beamwidth of a transmitter | ψ^r | Sector level beamwidth of the receiver |
| T_P | Pilot transmission time | T | Total transmission time |
| τ | Alignment time | g^t | Gain of transmitter |
| g^r | Gain of receiver | g^c | Channel gain |
| p_i | Power of the i th base station | E_f | Error frame |
| d_i | Data rate of the i th link | N | Noise |
| θ^t | Transmission angle | θ^r | Reception angle |
| E | Energy | r | Network rate |
| M | Maximum number of links | - | - |

In Equations (13) and (14), z is $0 < z \ll 1$. Considering transmission and reception gain, SINR can be evaluated by Equation (15).

$$SINR_i = \frac{p_i g_{i,i}^t g_{i,i}^c g_{i,i}^r}{\sum_{k=1, k \neq i}^M p_k g_{k,i}^t g_{k,i}^c g_{k,i}^r + n} \tag{15}$$

Then the network rate can be evaluated by (16) by using (15).

$$R_i = \left(1 - \frac{\tau_i}{T}\right) \log_2(1 + SINR_i) \tag{16}$$

Here, R_i signifies the i th link rate in the network, T represents the total transmission time, τ_i represents the time needed for the orientation of the i th link, while $SINR_i$ signifies the signal to noise and interference ratio of the corresponding i th link.

3.2.7. The Energy Efficiency (EE) of Network

The i th link EE is determined by Equation (17) [41].

$$EE_i = \frac{d_i}{p_i} \tag{17}$$

In Equation (17), E_i represents energy. d_i shows data rate of the i th link, and p_i denotes the power of the i th DBMS.

3.3. Objectives and Constraints

3.3.1. Objectives

The aim of our study is to increase the throughput as well as EE of the HetNet deployed in the InF.

3.3.2. First Objective

This objective is related to the maximum throughput in mm-waves- μ wave HetNets. This is mathematically described using Equation (18).

$$\max_{\varphi^t, \varphi^r, p, r} F1 = \sum_{i=1}^M R_i \tag{18}$$

$$\text{s.t. } \varphi_i^t \leq \psi_i^t, \quad 1 \leq i \leq M \tag{18a}$$

$$\varphi_i^r \leq \psi_i^r, \quad 1 \leq i \leq M \tag{18b}$$

$$0 \leq p_i \leq p^{max}, \quad 1 \leq i \leq M \tag{18c}$$

$$r_i \geq r^{max}, \quad 1 \leq i \leq M \tag{18d}$$

$$SINR_i \geq SINR^{max}, \quad 1 \leq i \leq M \tag{18e}$$

$$\varphi_i^t \varphi_i^r \geq \frac{T_p}{T} \psi_i^t \psi_i^r, \quad 1 \leq i \leq M \tag{18f}$$

3.3.3. Second Objective

The corresponding second objective of this work is to maximize EE in mm-waves-μ wave HetNets. This is mathematically described in Equation (19).

$$\max_{\varphi^t, \varphi^r, p, r} F2 = \sum_{i=1}^M EE_i \tag{19}$$

$$\text{s.t. } \varphi_i^t \leq \psi_i^t, \quad 1 \leq i \leq M \tag{19a}$$

$$\varphi_i^r \leq \psi_i^r, \quad 1 \leq i \leq M \tag{19b}$$

$$0 \leq p_i \leq p^{max}, \quad 1 \leq i \leq M \tag{19c}$$

$$r_i \geq r^{max}, \quad 1 \leq i \leq M \tag{19d}$$

$$SINR_i \geq SINR^{max}, \quad 1 \leq i \leq M \tag{19e}$$

$$\varphi_i^t \varphi_i^r \geq \frac{T_p}{T} \psi_i^t \psi_i^r, \quad 1 \leq i \leq M \tag{19f}$$

3.3.4. Constraints

1. According to Equations (18a) and (19a), for any *i*th transmitter, the sector level beamwidth must be greater than or equal to the beam level beamwidth.
2. According to Equations (18b) and (19b), for any *i*th receiver, the sector level beamwidth must be greater than or equal to the beam level beamwidth.
3. According to Equations (18c) and (19c), the maximum power level is always more significant than the power of any *i*th link.
4. According to the fourth constraints Equations (18d) and (19d), the rate of the *i*th link should be greater than the minimum rate for communication for successful communication.
5. According to the fifth constraint Equations (18e) and (19e), the SINR of the *i*th link should be higher than or equal to the minimum level of SINR.
6. The last constraint Equations (18f) and (19f) rationalize the corresponding lower bounds on the accessible bandwidth.

4. Proposed Algorithm

The performance analysis of throughput and EE in mm-wave-μ wave HetNet using OAA and heuristic algorithms is carried out in this section. At first, the algorithm is described, then modeled mathematically using (18) and (19), and correspondingly optimized utilizing OAA.

4.1. Outer Approximation Algorithm (OAA)

The problems in (18) and (19) are MINLP. These problems are very hard to solve due to their complexity, and exhaustive search achieves optimal solutions to these problems. However, it becomes complex when *M* increases. Therefore, we suggest an outer approximation algorithm (OAA) to resolve this problem. Figure 5 shows the flowchart of the OAA algorithm. Algorithm 1 explains the pseudo-code of OAA.

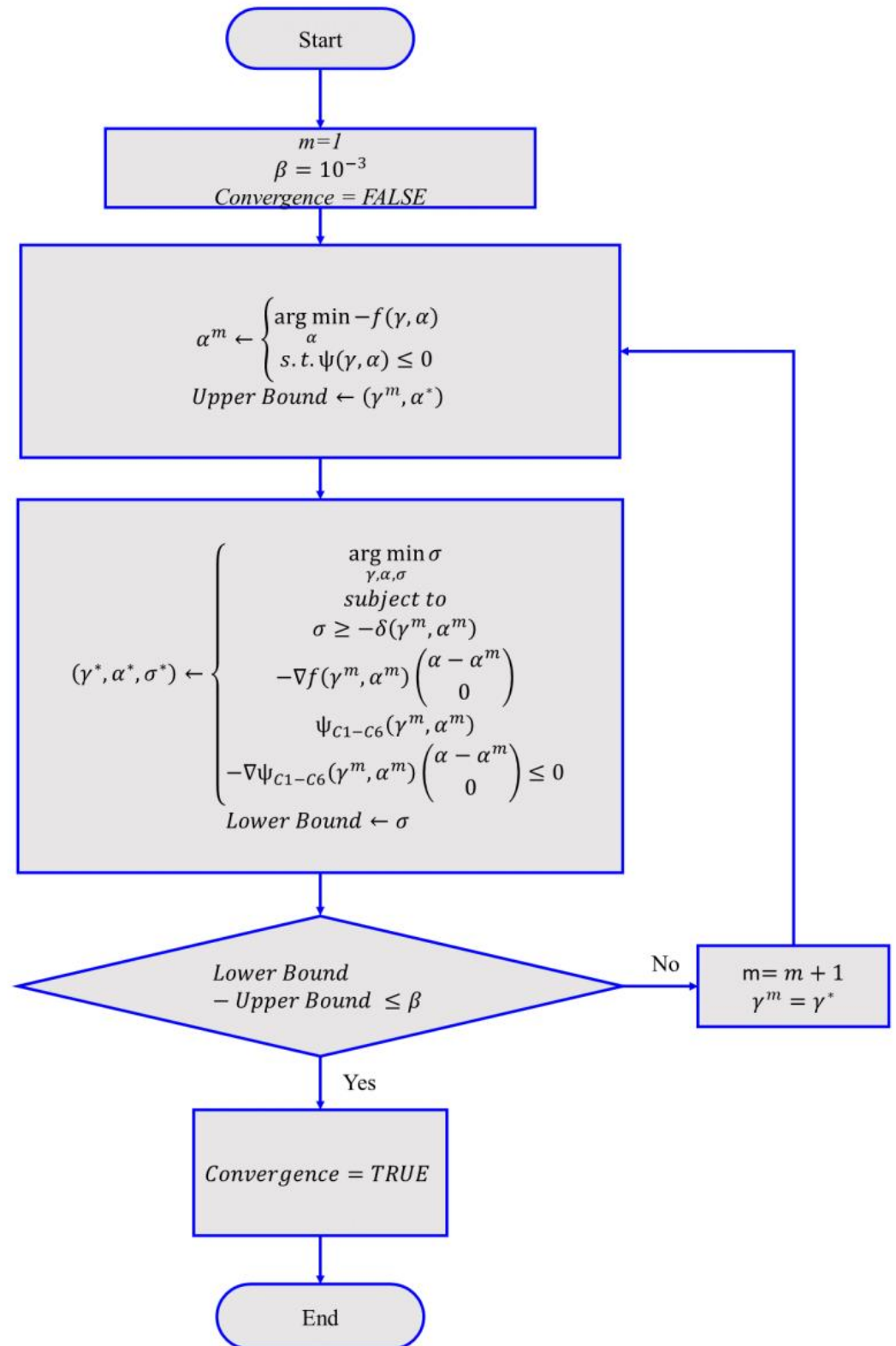


Figure 5. Flowchart of OAA algorithm.

Algorithm 1: Outer Approximation Algorithm

```

m ← 1
Initialize γ
β ← 10-3
Convergence ← FALSE
while Convergence == FALSE do
    αm ← { minα - f(γ, α)
           s.t. ψ(γ, α) ≤ 0;
    Upper Bound ← f(γm, α*)
    (γ*, α*, σ*) ← { minγ,σ,α σ
                    subject to
                    σ ≥ -δ(γm, αm)
                    -∇f(γm, αm) ( α - αm )
                    ψC1-C6(γm, αm)
                    -∇ψC1-C6(γm, αm) ( α - αm ) ≤ 0
    Lower Bound ← σ
    if Upper Bound - Lower Bound ≤ β then
        Convergence ← TRUE
    end
    else
        m ← m + 1
        γk ← γ*
    end
End

```

Explanation of the Algorithm

Let f be the corresponding objective, ψ_{C1-C6} signify constraints from C1 to C6 in Equations (18) and (19), $\alpha = \{P_{DBMS \text{ using } mm \text{ Waves}}, P_{DBMS \text{ using } Waves}\}$ and $\gamma = x \cup \alpha$. (19) fulfil the following propositions.

1. The objective function f and ψ_{C1-C6} are convex in α for a specified value of γ because α is nonempty, convex, and compact.
2. Continuous differentiation of objective function f and ψ_{C1-C6} must be possible.
3. By fixing the value of γ , the solution of every non-linear continuous sub-problem qualifies the constraints.
4. After solving γ , the appropriate solution NLP problem is obtained.

These assumptions convert Equations (18) and (19) into unique problems. OAA provides the solution to these master problems. The separation of objective function f and the constrained constraints of convex directs to external measurements. The OAA utilizes high limits and low-frequency sequences to fulfil proposals, as indicated above, for corresponding mixed problems. OAA achieves optimal value when β converges. A problem that does not match the line has a higher sequence. The main problem can be written as

$$\begin{cases} \min_{\alpha} - f(\gamma, \alpha) \\ \text{s.t. } \psi(\gamma, \alpha) \leq 0; \end{cases} \tag{20}$$

The solution to (20) is α^m , and it is used for the master problem. The upper bounds can be obtained from the primary concern, while the lower bounds can be achieved by solving the master problem. The first solution α is used to drive the master problem. The solution to the master problem presents a new set of variables γ^{m+1} . As the iteration progresses, the upper and lower limits come together. The algorithm terminates when both boundaries are

close such that their difference is less than β . The master problem can be extracted in two steps. Initially, an issue that has been created in a total space γ is labelled as:

$$\begin{cases} \min_{\gamma} \min_{\alpha} -f(\gamma^m, \alpha) \\ \text{s.t. } \psi(\gamma^m, \alpha) \leq 0; \end{cases} \tag{21}$$

The above problem is expressed as

$$\min_{\gamma} -\theta(\gamma) \tag{22}$$

here

$$\begin{cases} \theta(\gamma) = \min_{\alpha} -f(\gamma^m, \alpha) \\ \text{s.t. } \psi(\gamma^m, \alpha) \leq 0; \end{cases} \tag{23}$$

The projection of the problem in (18) and (19) using discrete variable γ is expressed as a problem (22). The outer approximation can be made by applying linearization in the second step. Therefore, the solution to the projection problem is:

$$\begin{cases} \min_{\gamma} \min_{\alpha} -f(\alpha^m, \gamma^m) - \nabla f(\alpha^m, \gamma^m) \begin{pmatrix} \alpha - \alpha^m \\ \gamma - \gamma^m \end{pmatrix} \\ \text{s.t. } -\psi(\alpha^m, \gamma^m) - \nabla \psi(\alpha^m, \gamma^m) \begin{pmatrix} \alpha - \alpha^m \\ \gamma - \gamma^m \end{pmatrix} \end{cases} \tag{24}$$

With the introduction of new variables, the optimization problem can be expressed as:

$$\begin{aligned} & \text{minimum}_{\gamma, \alpha, \sigma} \sigma \\ \text{s.t. : } & \begin{cases} \sigma \geq -f(\alpha^m, \gamma^m) - \nabla f(\alpha^m, \gamma^m) \begin{pmatrix} \alpha - \alpha^m \\ \gamma - \gamma^m \end{pmatrix} \\ -\psi(\alpha^m, \gamma^m) - \nabla \psi(\alpha^m, \gamma^m) \begin{pmatrix} \alpha - \alpha^m \\ \gamma - \gamma^m \end{pmatrix} \leq 0 \end{cases} \end{aligned} \tag{25}$$

The above master problem provides lower bounds. The projection of the issues in (18) and (19) is the problem formulated in (25). The problem is a linear mixed-integer programming problem (MILP), and the iterative method solves it. The following section explains the results obtained by the simulation of the proposed algorithm.

5. Results and Experiments

The system model is simulated in MATLAB 2021Ra using the OPTI toolbox. The experimental results obtained from the simulations are shown in this section, and the outcomes also explain the usefulness and the convergence of the corresponding algorithm. The experimental results of the proposed algorithm are also compared with the state-of-the-art algorithms. The performance analysis of the network is calculated in terms of throughput, EE, link rate, and channel efficiency.

Simulation Parameters

The values of the different parameters employed to simulate the system model are demonstrated in Table 4. The simulation parameters of the other algorithms are illustrated in Appendix A Table A1.

Table 4. Simulation parameters of each base station.

| Parameter | Value |
|-----------------|----------------------|
| DBMS power, p | 25 Watts |
| Minimum users | 2 |
| Maximum users | 50 |
| UE increment | 2 |
| T_p | 20 μ seconds |
| T | 65,535 μ seconds |

We have used two algorithms, namely OAA and NOMAD [38], to increase the throughput and corresponding EE. Figure 6 demonstrates the throughput using OAA. Additionally, it reveals that it increases with the corresponding number of UEs. Likewise, Figure 7 shows the EE using the OAA. It indicates that the output converges as UEs rise. By increasing the UEs, average EE increases. When the number of users is 18, the average EE of the network is 4.5 Mbits/J; it remains approximately 4.5 Mbits/J until the number of users reaches 46. After 46 users, the interference dominates, and the EE decreases. This is due to the congestion of the UEs in the hall, as for the successful operation the hall should have less than 60% density according to 3GPP InF scenario.

Figure 8 shows the distribution of users on mm-waves and μ waves when the OAA algorithm is applied. Initially, when the total number of users is two, then one user is on mm-waves while the other is on μ waves. With the increment in users, the distribution does not remain symmetrical; μ waves users become more significant, such as when the number of users is 34, and mm-waves users are 20 while μ waves users are 14. The procedure for selecting a particular mode depends on several factors. For the selection of mm-wave mode, the sparse density should be less than 40%, and there should be enough possibility to have LOS for a more significant duration while the sparse density is greater than 40% for microwave mode.

We have also calculated the variations in the link rates by changing SINR. Figure 9 shows the plot between SINR in decibels (dB) and link rate (Mbps) and the link rate of mm-wave link is better than μ wave link. When SINR is 40 dB, the link rate of mm-wave link approaches 60 Mbps while the link rate of μ wave link approaches 42 Mbps which is relatively low compared to mm-wave link.

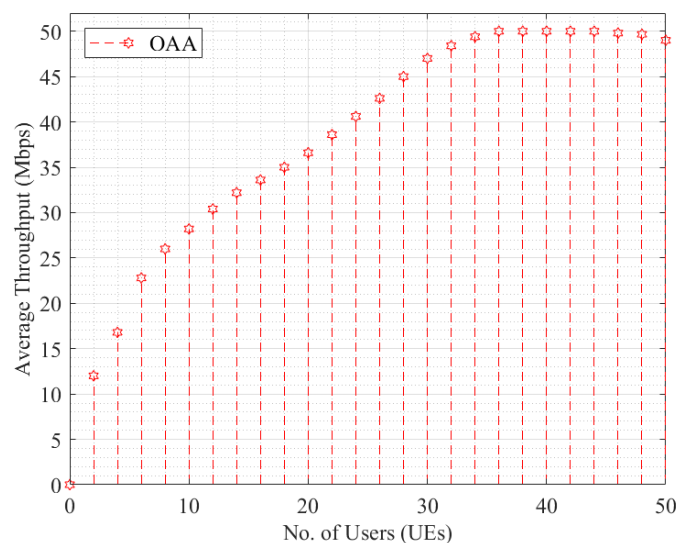


Figure 6. The number of users vs. corresponding average throughput.

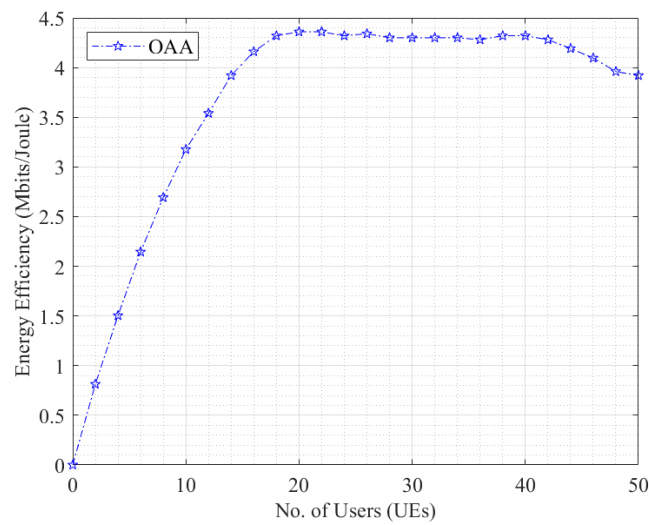


Figure 7. The number of users vs. corresponding average energy efficiency.

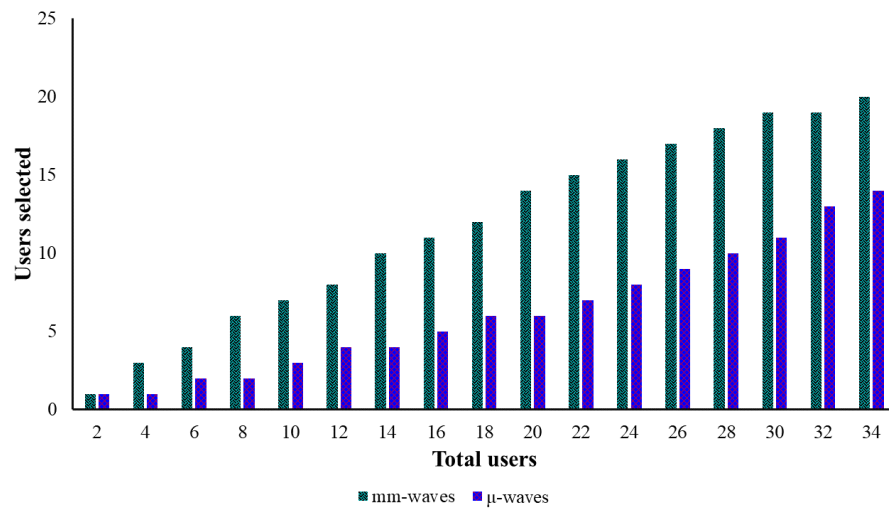


Figure 8. Selected users on mm-waves and μ waves.

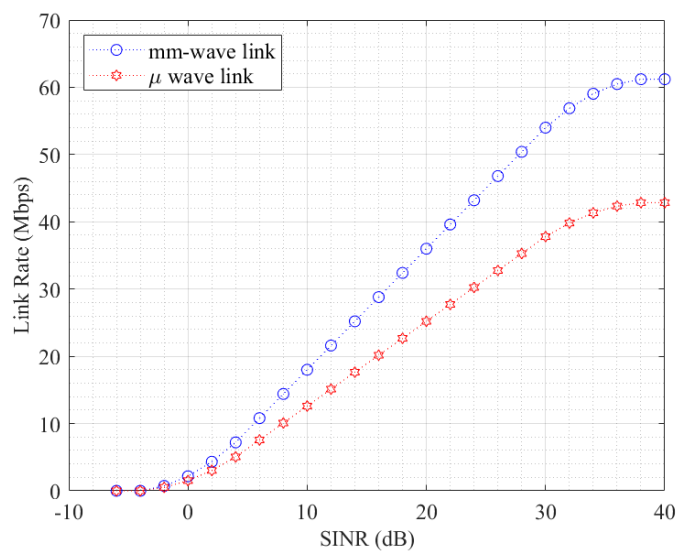


Figure 9. SINR vs Link Rate of mm-waves and μ waves.

We have evaluated the performance of the proposed algorithm in the case of LOS, NLOS and HetNet scenarios. Figure 10 illustrates the relationship between the average throughput of the network and the number of users for the LOS, NLOS, and HetNet scenarios. From the plot, the optimal performance from the proposed HetNet scheme using the OAA algorithm.

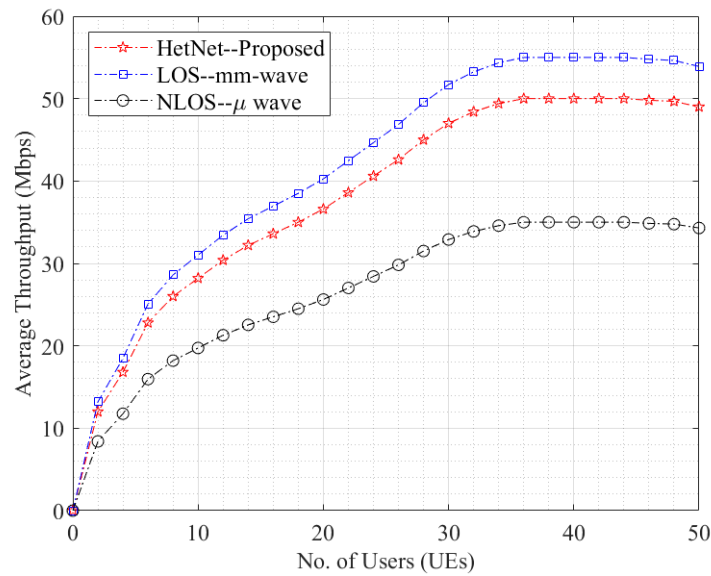


Figure 10. Throughput vs No. of UEs for LOS, NLOS, and HetNet.

Similarly, we have calculated the relationship between energy efficiency and the number of users for the LOS, NLOS, and HetNets scenario using the OAA algorithm. Figure 11 shows the plot of energy efficiency against the number of users for all three designs. When there is LOS, the communication is very smooth and maximum throughput is achieved using mm-wave. However, when there is NLOS, and microwaves are used then the performance of the network is relatively worse than the proposed HetNet which shows optimal performance and works in both LOS and NLOS scenarios.

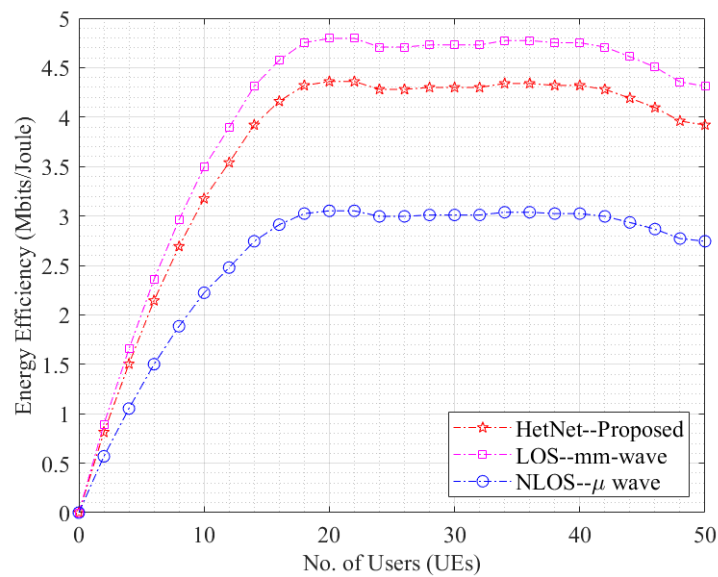


Figure 11. Energy Efficiency vs No. of UEs for LOS, NLOS and HetNet.

We also compare the performance of the proposed algorithm OAA and other existing algorithms regarding EE and throughput of the network. Figure 12 illustrates the average EE of the system when all the algorithms are applied. The plot curves show that all other algorithms converge slowly, and the maximum average EE achieved by the GA algorithm is more petite than OAA, i.e., approximately 4.2 Mbits/J. In contrast to all these algorithms, the OAA has a better convergence rate, and it provides a better average EE of the network, i.e., 4.5 Mbits/J. These observations from Figure 12 show that OAA is better than existing optimization algorithms.

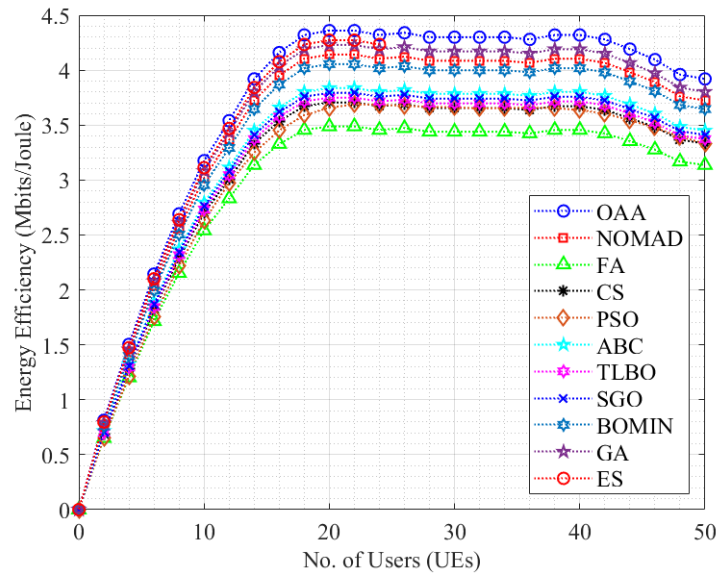


Figure 12. Average EE of network with OAA and other algorithms.

We also compare the performance of both algorithms regarding the throughput of the network, as shown in Figure 13. When the total users are two, the network throughput with the OAA algorithm is 12 Mbps, while GA is 10 Mbps. Throughput varies directly with the entire users, but the network’s throughput with OAA remains better than NOMAD when users are approaching the upper limit, i.e., 50. The average throughput of the network is 50 Mbps with OAA and 48 Mbps with GA.

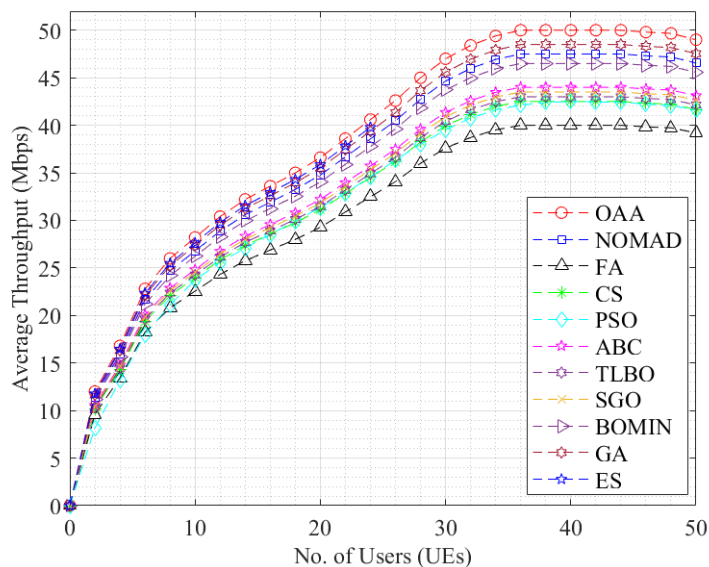


Figure 13. Average throughput of the network with OAA and other algorithms.

After all of the experiments, we find that the performance of the OAA is better than algorithms. Finally, we have calculated the relationship between throughput and channel efficiency of the network using the OAA algorithm. Figure 14 shows the plot between channel efficiency and throughput in LOS and NLOS.

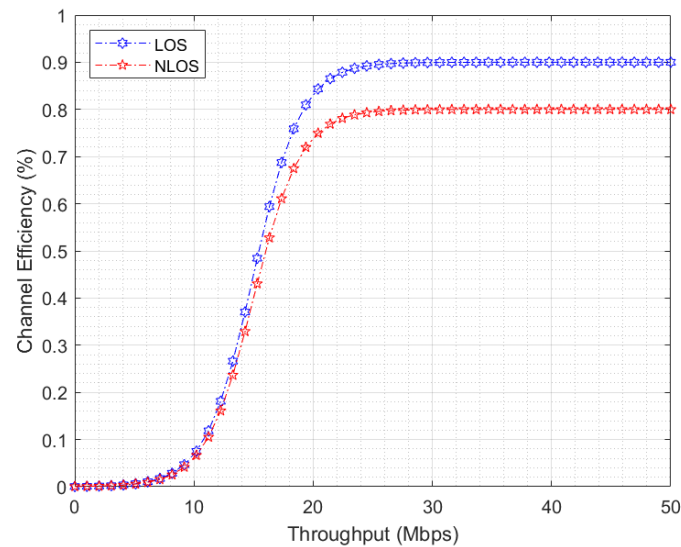


Figure 14. Channel efficiency vs throughput of the network with OAA.

We have also compared the optimal solution of the proposed algorithm with the other algorithms in terms of EE and throughput. Table 5 highlights the optimal solution of all the algorithms.

Table 5. Comparison of the optimal solution of proposed algorithm with the existing algorithms.

| Algorithm | Optimal EE (Mbj ⁻¹) | Gain in the EE | Optimal Throughput (Mbps) | Gain in the Throughput |
|-----------|---------------------------------|----------------|---------------------------|------------------------|
| OAA | 4.50 | | 50.00 | |
| NOMAD | 4.10 | | 46.93 | |
| FA | 3.46 | | 39.52 | |
| CS | 3.67 | | 41.99 | |
| PSO | 3.59 | 7.4% | 41.61 | 4.34% |
| ABC | 3.80 | | 43.47 | |
| TLBO | 3.71 | | 42.48 | |
| SGO | 3.75 | | 42.98 | |
| BOMIN | 4.01 | | 45.94 | |
| GA | 4.19 | | 47.92 | |

We have also evaluated the runtime complexity of the proposed algorithm with other existing algorithms and summarized in Table 6. All the runtime complexities are evaluated on the CPU core i5 (Intel, Chandler, AZ, USA) and GPU Tesla K80 (NVIDIA, Santa Clara, CA, USA).

Table 6. Comparison of the runtime complexity of the proposed algorithm with others.

| Algorithm | Runtime Complexity (GPU) | Difference | Overall Gain | Runtime Complexity (CPU) | Difference | Overall Gain |
|-----------|--------------------------|------------|--------------|--------------------------|------------|--------------|
| OAA | 0.8 s | 0s | 47.06% | 46 s | 0 s | 45.10% |
| NOMAD | 4 s | 3.2 s | | 224 s | 178 s | |
| FA | 3 s | 2.2 s | | 168 s | 122 s | |
| CS | 6 s | 5.2 s | | 336 s | 290 s | |
| PSO | 2.5 s | 1.7 s | | 90 s | 44 s | |
| ABC | 1.7 s | 0.9 s | | 102 s | 56 s | |
| TLBO | 5 s | 4.2 s | | 280 s | 234 s | |
| SGO | 9 s | 8.2 s | | 504 s | 458 s | |
| BOMIN | 11 s | 10.2 s | | 616 s | 570 s | |
| GA | 4 s | 3.2 s | | 224 s | 178 s | |
| ES | 30 s | 29.2 s | | 1680 s | 1634 s | |

6. Conclusions

We have analyzed the problem of throughput and corresponding energy efficiency in mm-wave- μ waves HetNets. We studied the problem of the concave fractional system. We suggest OAA resolves the issue. The proposed algorithm varies sequentially and gives good results within $\beta = 10^{-3}$. The performance of the β -optimal solution obtained by the OAA method is indicated by different system parameters such as the number of users and network input. EE improves as the total users increase and become more stable as we grow UEs again. The average throughput increases with the increase in the number of users, and with the rise in users, more users switch to μ wave links. The optimal throughput obtained by the proposed algorithm is 50 Mbps, while the optimal energy efficiency achieved by the proposed algorithm is 4.5 Mbits/J. The proposed algorithm applies to millimeter-waves microwaves heterogeneous networks within the defined area, as in the case of the indoor factory. In future, we will extend this to metropolitan area networks. We will also use more robust artificial intelligence and machine learning algorithms to make the network perform well in different environments rather than focusing on the only indoor factory.

Author Contributions: Conceptualization, S.J. and M.R.; methodology, S.J.; software, S.J. and J.T.; validation, M.R. and A.H.; formal analysis, S.J.; investigation, M.R.; resources, M.R.; data curation, S.J. and J.T.; writing—original draft preparation, S.J.; writing—review and editing, M.R. and J.T.; visualization, M.R.; supervision, A.H.; project administration, A.H.; and funding acquisition, A.H. All authors have read and agreed to the published version of the manuscript.

Funding: This research received no external funding.

Conflicts of Interest: The authors declare no conflict of interest.

Appendix A

The simulation parameters of the other algorithms are summarized in Table A1.

Table A1. Simulation parameters of the other algorithms.

| Algorithm | Parameters | Values |
|-----------|---------------|----------------------|
| NOMAD | DBMS power, p | 25 Watts |
| | Minimum users | 2 |
| | Maximum users | 50 |
| | UE increment | 2 |
| | T_P | 20 μ seconds |
| | T | 65,535 μ seconds |
| FA | DBMS power | 25 Watts |
| | Minimum rate | 1 kbps |
| | T_P | 20 μ seconds |
| | T | 65,535 μ seconds |
| CS | DBMS power | 25 Watts |
| | Minimum rate | 1 kbps |
| | T_P | 20 μ seconds |
| | T | 65,535 μ seconds |
| PSO | Bandwidth | 180 kHz |
| | DBMS power | 25 Watts |
| | Minimum rate | 1 kbps |
| | Maximum users | 50 |
| | Minimum users | 2 |
| | T_P | 20 μ seconds |
| | T | 65,535 μ seconds |
| ABC | Bandwidth | 180 kHz |
| | DBMS power | 25 Watts |
| | Minimum rate | 1 kbps |
| | T_P | 20 μ seconds |
| TLBO | T | 65,535 μ seconds |
| | DBMS power | 25 Watts |
| | Minimum rate | 1 kbps |
| | Pilot time | 30 μ seconds |
| SGO | Bandwidth | 180 kHz |
| | DBMS power, p | 25 Watts |
| | Minimum users | 2 |
| | Maximum users | 50 |
| | UE increment | 2 |
| | T_P | 20 μ seconds |
| | T | 65,535 μ seconds |

Table A1. Cont.

| Algorithm | Parameters | Values |
|-----------|---------------|----------------------|
| BOMIN | DBMS power, p | 25 Watts |
| | Minimum users | 2 |
| | Maximum users | 50 |
| | UE increment | 2 |
| | T_P | 50 μ seconds |
| | T | 65,535 μ seconds |
| GA | DBMS power | 25 Watts |
| | Minimum rate | 1 kbps |
| | Pilot time | 40 μ seconds |
| | Bandwidth | 180 kHz |

References

- Rappaport, T.S.; Sun, S.; Mayzus, R.; Zhao, H.; Azar, Y.; Wang, K.; Wong, G.N.; Schulz, J.K.; Samimi, M.; Gutierrez, F. Millimeter Wave Mobile Communications for 5G Cellular: It will Work! *IEEE Access* **2013**, *1*, 335–349. [[CrossRef](#)]
- Haider, A.; Rahman, M.; Khan, T.; Niaz, M.T.; Kim, H.S. Multi-Gigabit Co-OFDM System over SMF and MMF Links for 5G URLLC Backhaul Network. *Comput. Mater. Contin.* **2021**, *67*, 1747–1758. [[CrossRef](#)]
- Fawad Khan, M.J.; Rahman, M.; Amin, Y.; Tenhunen, H. Low-Rank Multi-Channel Features for Robust Visual Object Tracking. *Symmetry* **2019**, *11*, 1155. [[CrossRef](#)]
- Perfecto, C.; Del Ser, J.; Bennis, M. Millimeter-Wave V2V Communications: Distributed Association and Beam Alignment. *IEEE J. Sel. Areas Commun.* **2017**, *35*, 2148–2162. [[CrossRef](#)]
- Jamil, S.; Fawad; Rahman, M.; Ullah, A.; Badnava, S.; Forsat, M.; Mirjavadi, S.S. Malicious UAV Detection Using Integrated Audio and Visual Features for Public Safety Applications. *Sensors* **2020**, *20*, 3923. [[CrossRef](#)]
- Agiwal, M.; Roy, A.; Saxena, N. Next Generation 5G Wireless Networks: A Comprehensive Survey. *IEEE Commun. Surv. Tutor.* **2016**, *18*, 1617–1655. [[CrossRef](#)]
- Ansari, R.I.; Pervaiz, H.; Chrysostomou, C.; Hassan, S.A.; Mahmood, A.; Gidlund, M. Control-Data Separation Architecture for Dual-Band mm wave Networks: A New Dimension to Spectrum Management. *IEEE Access* **2019**, *7*, 34925–34937. [[CrossRef](#)]
- Haider, A.; Khan, M.A.; Rehman, A.; Rahman, M.U.; Kim, H.S. A Real-Time Sequential Deep Extreme Learning Machine Cybersecurity Intrusion Detection System. *Comput. Mater. Contin.* **2021**, *66*, 1785–1798. [[CrossRef](#)]
- Kim, D.; Choi, M. Non-Orthogonal Multiple Access in Distributed Antenna Systems for Max-Min Fairness and Max-Sum-Rate. *IEEE Access* **2021**, *9*, 69467–69480. [[CrossRef](#)]
- Xu, L.; Zhou, X.; Tao, Y.; Liu, L.; Yu, X.; Kumar, N. Intelligent Security Performance Prediction for IoT-Enabled Healthcare Networks Using an Improved CNN. *IEEE Trans. Ind. Inform.* **2022**, *18*, 2063–2074. [[CrossRef](#)]
- Chergui, H.; Tourki, K.; Lguensat, R.; Benjillali, M.; Verikoukis, C.V.; Debbah, M. Classification Algorithms for Semi-Blind Uplink/Downlink Decoupling in Sub-6 GHz/mmWave 5G Networks. In Proceedings of the 2019 15th International Wireless Communications and Mobile Computing Conference (IWCMC), Tangier, Morocco, 24–28 June 2019; pp. 2031–2035.
- Semiari, O.; Saad, W.; Bennis, M. Joint Millimeter Wave and Microwave Resources Allocation in Cellular Networks with Dual Mode Base Stations. *IEEE Trans. Wirel. Commun.* **2017**, *16*, 4802–4816. [[CrossRef](#)]
- Semiari, O.; Saad, W.; Bennis, M.; Debbah, M. Integrated Millimeter Wave and Sub-6 GHz Wireless Networks: A Roadmap for Joint Mobile Broadband and Ultra-Reliable Low-Latency Communications. *IEEE Wirel. Commun.* **2019**, *26*, 109–115. [[CrossRef](#)]
- Shokri-Ghadikolaei, H.; Gkatzikis, L.; Fischione, C. Beamsearching and transmission scheduling in millimeter wave communications. In Proceedings of the 2015 IEEE International Conference on Communications (ICC), London, UK, 8–12 June 2015; pp. 1292–1297.
- Mismar, F.B.; Evans, B.L. Partially Blind Handovers for mm wave New Radio Aided by Sub-6 GHz LTE Signaling. In Proceedings of the 2018 IEEE International Conference on Communications Workshops, Kansas City, MO, USA, 20–24 May 2018; pp. 1–5.
- Okamoto, H.; Nishio, T.; Morikura, M.; Yamamoto, K.; Murayama, D.; Nakahira, K. Machine-Learning-Based Throughput Estimation Using Images for mmWave Communications. In Proceedings of the 2017 IEEE 85th Vehicular Technology Conference (VTC Spring), Sydney, NSW, Australia, 4–7 June 2017; pp. 1–6.
- Math, S.; Tam, P.; Kim, S. Reliable Federated Learning Systems Based on Intelligent Resource Sharing Scheme for Big Data Internet of Things. *IEEE Access* **2021**, *9*, 108091–108100. [[CrossRef](#)]
- Niknam, S.; Nasir, A.A.; Mehrpouyan, H.; Natarajan, B. A Multiband Ofdma Heterogeneous Network for Millimeter Wave 5G Wireless Applications. *IEEE Access* **2016**, *4*, 5640–5648. [[CrossRef](#)]

19. Haider, A.; Rahman, M.; Ahmad, H.; NaghshvarianJahromi, M.; Niaz, M.T.; Kim, H.S. Frequency-Agile WLAN Notch UWB Antenna for URLLC Applications. *Comput. Mater. Contin.* **2021**, *67*, 2243–2254. [[CrossRef](#)]
20. Fadel, A.; Cousin, B.; Khalil, A. User Selection in 5G Heterogeneous Networks Based on Millimeter-Wave and Beamforming. In Proceedings of the 2018 IEEE 20th International Conference on High Performance Computing and Communications; IEEE 16th International Conference on Smart City; IEEE 4th International Conference on Data Science and Systems (HPCC/SmartCity/DSS), Exeter, UK, 28–30 June 2018; pp. 503–509.
21. Munir, H.; Pervaiz, H.; Hassan, S.A.; Musavian, L.; Ni, Q.; Imran, M.A.; Tafazolli, R. Computationally Intelligent Techniques for Resource Management in mm wave Small Cell Networks. *IEEE Wirel. Commun.* **2018**, *25*, 32–39. [[CrossRef](#)]
22. Busari, S.A.; Huq, K.M.S.; Felfel, G.; Rodriguez, J. Adaptive resource allocation for energy-efficient millimeter-wave massive mimo networks. In Proceedings of the 2018 IEEE Global Communications Conference (GLOBECOM), Abu Dhabi, United Arab Emirates, 9–13 December 2018; pp. 1–6.
23. Hao, W.; Zeng, M.; Chu, Z.; Yang, S.; Sun, G. Energy-Efficient Resource Allocation for mm wave Massive MIMO HetNets with Wireless Backhaul. *IEEE Access* **2018**, *6*, 2457–2471. [[CrossRef](#)]
24. Zeng, M.; Hao, W.; Dobre, O.A.; Poor, H.V. Energy-Efficient Power Allocation in Uplink mm wave Massive MIMO with NOMA. *IEEE Trans. Veh. Technol.* **2019**, *68*, 3000–3004. [[CrossRef](#)]
25. Pu, W.; Li, X.; Yuan, J.; Yang, X. Resource Allocation for Millimeter Wave Self-Backhaul Network using Markov Approximation. *IEEE Access* **2019**, *7*, 61283–61295. [[CrossRef](#)]
26. Shi, J.; Xiao, P.; Kelly, J.; Si, J. Resource Allocation and Interference Management in Hybrid Millimeter Wave Networks. In Proceedings of the 2017 IEEE/CIC International Conference on Communications in China (ICCC), Qingdao, China, 22–24 October 2017; pp. 1–6.
27. Chaieb, C.; Mlika, Z.; Abdelkefi, F.; Ajib, W. On The User Association and Resource Allocation in HetNets With mm wave Base Stations. In Proceedings of the 2017 IEEE 28th Annual International Symposium on Personal, Indoor, and Mobile Radio Communications (PIMRC), Montreal, QC, Canada, 8–13 October 2017; pp. 1–5.
28. Jamil, S.; Rahman, M.; Haider, A. Bag of Features (BoF) Based Deep Learning Framework for Bleached Corals Detection. *Big Data Cogn. Comput.* **2021**, *5*, 53. [[CrossRef](#)]
29. Mesodiakaki, A.; Adelantado, F.; Alonso, L.; Di Renzo, M.; Verikoukis, C. Energy- and Spectrum-Efficient User Association in Millimeter-Wave Backhaul Small-Cell Networks. *IEEE Trans. Veh. Technol.* **2017**, *66*, 1810–1821. [[CrossRef](#)]
30. Mesodiakaki, A.; Zola, E.; Kassler, A. User association in 5G heterogeneous networks with mesh millimeter wave backhaul links. In Proceedings of the 2017 IEEE 18th International Symposium on a World of Wireless, Mobile and Multimedia Networks (WoWMoM), Macau, China, 12–15 June 2017; pp. 1–6.
31. Selvakumar, B.; Muneeswaran, K. Firefly Algorithm-Based Feature Selection for Network Intrusion Detection. *Comput. Secur.* **2019**, *81*, 148–155.
32. Mareli, M.; Twala, B. An Adaptive Cuckoo Search Algorithm for Optimization. *Appl. Comput. Inform.* **2018**, *14*, 107–115. [[CrossRef](#)]
33. Sengupta, S.; Basak, S.; Peters, R.A., II. Particle swarm optimization: A survey of historical and recent developments with hybridization perspectives. *Mach. Learn. Knowl. Extr.* **2019**, *1*, 157–191. [[CrossRef](#)]
34. Xu, X.; Hao, J.; Zheng, Y. Multi-Objective Artificial Bee Colony Algorithm for Multi-Stage Resource Leveling Problem in Sharing Logistics Network. *Comput. Ind. Eng.* **2020**, *142*, 106338. [[CrossRef](#)]
35. Zou, F.; Chen, D.; Xu, Q. A Survey of Teaching Learning-Based Optimization. *Neurocomputing* **2019**, *335*, 366–383. [[CrossRef](#)]
36. Praveen, S.P.; Rao, K.T.; Janakiramaiah, B. Effective Allocation of Resources and Task Scheduling in Cloud Environment using Social Group Optimization. *Arab. J. Sci. Eng.* **2018**, *43*, 4265–4272. [[CrossRef](#)]
37. Cimorelli, L.; Fecarotta, O. Optimal Regulation of Variable Speed Pumps in Sewer Systems. *Environ. Sci. Proc.* **2020**, *2*, 2058. [[CrossRef](#)]
38. Guerrero, C.; Lera, I.; Juiz, C. Genetic Algorithm for Multi-Objective Optimization of Container Allocation in Cloud Architecture. *J. Grid Comput.* **2018**, *16*, 113–135. [[CrossRef](#)]
39. Ayesha, A.; Rahman, M.; Haider, A.; Majeed Chaudhry, S. On Self-Interference Cancellation and Non-Idealities Suppression in Full-Duplex Radio Transceivers. *Mathematics* **2021**, *9*, 1434. [[CrossRef](#)]
40. Ahmed, N.M.; Rikli, N.E. QoS-based Data Aggregation and Resource Allocation Algorithm for Machine Type Communication Devices in Next-Generation Networks. *IEEE Access* **2021**, *9*, 119735–119754. [[CrossRef](#)]
41. Ali, S.; Haider, A.; Rahman, M.; Sohail, M.; Zikria, Y.B. Deep Learning (DL) based Joint Resource Allocation and RRH Association in 5G-multi-tier Networks. *IEEE Access* **2021**, *9*, 118357–118366. [[CrossRef](#)]